

## RESEARCH ARTICLE

# Assessment of airway response distribution and paradoxical airway dilation in mice during methacholine challenge

S. Dubsky,<sup>1</sup> G. R. Zosky,<sup>2</sup> K. Perks,<sup>3</sup> C. R. Samarage,<sup>1,4</sup> Y. Henon,<sup>1,4</sup> S. B. Hooper,<sup>5,6</sup> and A. Fouras<sup>1,4</sup>

<sup>1</sup>Department of Mechanical and Aerospace Engineering, Monash University, Melbourne, Victoria, Australia; <sup>2</sup>School of Medicine, University of Tasmania, Hobart, Tasmania, Australia; <sup>3</sup>Harry Perkins Institute for Medical Research, The University of Western Australia, Nedlands, Western Australia, Australia; <sup>4</sup>4Dx Limited, Melbourne, Victoria, Australia; <sup>5</sup>The Ritchie Centre, Hudson Institute of Medical Research, Melbourne, Victoria, Australia; and <sup>6</sup>Department of Obstetrics and Gynaecology, Monash University, Melbourne, Victoria, Australia

Submitted 25 May 2016; accepted in final form 21 December 2016

**Dubsky S, Zosky GR, Perks K, Samarage CR, Henon Y, Hooper SB, Fouras A.** Assessment of airway response distribution and paradoxical airway dilation in mice during methacholine challenge. *J Appl Physiol* 122: 503–510, 2017. First published December 29, 2016; doi:10.1152/jappphysiol.00476.2016.—Detailed information on the distribution of airway diameters during bronchoconstriction in situ is required to understand the regional response of the lungs. Imaging studies using computed tomography (CT) have previously measured airway diameters and changes in response to bronchoconstricting agents, but the manual measurements used have severely limited the number of airways measured per subject. Hence, the detailed distribution and heterogeneity of airway responses are unknown. We have developed and applied dynamic imaging and advanced image-processing methods to quantify and compare hundreds of airways in vivo. The method, based on CT, was applied to house dust-mite-sensitized and control mice during intravenous methacholine (MCh) infusion. Airway diameters were measured pre- and post-MCh challenge, and the results compared demonstrate the distribution of airway response throughout the lungs during mechanical ventilation. Forced oscillation testing was used to measure the global response in lung mechanics. We found marked heterogeneity in the response, with paradoxical dilation of airways present at all airway sizes. The probability of paradoxical dilation decreased with decreasing baseline airway diameter and was not affected by pre-existing inflammation. The results confirm the importance of considering the lung as an entire interconnected system rather than a collection of independent units. It is hoped that the response distribution measurements can help to elucidate the mechanisms that lead to heterogeneous airway response in vivo.

**NEW & NOTEWORTHY** Information on the distribution of airway diameters during bronchoconstriction in situ is critical for understanding the regional response of the lungs. We have developed an imaging method to quantify and compare the size of hundreds of airways in vivo during bronchoconstriction in mice. The results demonstrate large heterogeneity with both constriction and paradoxical dilation of airways, confirming the importance of considering the lung as an interconnected system rather than a collection of independent units.

airways; methacholine; tomography; synchrotron imaging; mice

THE RESPONSE OF AIRWAYS to bronchoconstricting agents is a complex process that is not well understood. An individual

airway's response is determined by a variety of factors, including mechanical forces, intrinsic airway smooth muscle properties, airway smooth muscle tone, and the local inflammatory milieu. Modeling has demonstrated effects from the interdependence of airways (29), agonist-response interactions (1), and integrated tissue mechanics (22) that lead to heterogeneous airway response within the airway tree. Although in vitro studies have allowed us to understand the fundamental mechanisms of the response of isolated airways (5, 6, 20), in vivo studies are necessary to understand the dynamic response of the entire airway tree, which can exhibit complicated emergent behavior.

Imaging methods, in particular, computed tomography (CT), have been used to study airway response to airway constrictors in humans (17) and various animal models (3, 4, 27). These studies have confirmed a heterogeneous response of the airways in situ and identified paradoxical dilation of some airways in a number of species and in response to a range of bronchoconstricting interventions (3, 4, 17, 27). However, the manual processing methods used to measure the airway size in these studies were limited to measurements of between 6 segments (3) and 26 segments (17) per subject. This limited sample may not provide detailed information of the distribution of airway responses within the whole lung, and no studies have identified the distribution of response across the entire lung. This detailed information is required to understand better the dynamic response of the airway tree to bronchoconstriction and the as-yet-unidentified mechanisms involved in paradoxical dilation of the airways. Here, we present a method based on synchrotron phase-contrast CT that allows hundreds of airways to be digitally segmented, measured, and compared within the mouse lung. This allows us to quantify effectively the distribution of airway responses within the lung during breathing.

The aim of this study was to quantify regional constriction in the airways across the lung in response to bronchoconstriction, with and without prior airway inflammation. To achieve this, we measured the distribution of responses of the airways in house dust-mite (HDM)-sensitized and control (CTL) mice in response to two doses of intravenously (IV) infused methacholine (MCh). The MCh doses were chosen to produce a modest global response to assess the inherent airway response without introducing physiological complications or distress and additionally, to increase the likelihood of producing paradoxical

Address for reprint requests and other correspondence: S. Dubsky, Dept. of Mechanical & Aerospace Engineering, Monash Univ., Clayton, Victoria, Australia 3800 (e-mail: Stephen.Dubsky@monash.edu).

dilation. We also assessed lung mechanics using the forced oscillation technique (FOT) to determine the global effect of heterogeneous regional bronchoconstriction. By assessing the distribution of airway responses to an IV-infused bronchoconstricting agent, we avoid differential responses caused by variable exposure of the agonist to the airway smooth muscle when delivered via the airway lumen. By assessing the response in the presence and absence of prior exposure to the allergen (HDM), we were also able to investigate the effect of prior inflammation on the distribution of airway responses.

## MATERIALS AND METHODS

**Animal procedure.** All animal procedures were approved by the SPring-8 Animal Care Committee and the Animal Ethics Committee of Monash University's School of Biomedical Science. All studies were conducted in Experimental Hutch 3 of Beamline BL20B2 in the Biomedical Imaging Centre at the SPring-8 synchrotron in Japan.

Adult male Balb/c mice were lightly sedated with methoxyflurane and intranasally exposed to 25  $\mu\text{g}$  HDM ( $n = 5$ ) extract (Greer Laboratories, Lenoir, NC) in 50  $\mu\text{l}$  saline or saline alone (CTL;  $n = 5$ ). Mice were treated daily for 10 days and studied 24 h after the last exposure.

Each animal was anesthetized using sodium pentobarbitone (70 mg/kg ip), tracheostomized, and connected to a ventilator and a tail-vein catheter inserted for MCh infusion. Anesthesia was maintained throughout the experiment with top-up of sodium pentobarbitone every 30 min (30 mg/kg ip). Positive pressure ventilation was delivered through a custom-designed ventilator [based on that described in Kitchen et al. (16)] with 120 ms inspiration time, 280 ms expiration time, 10 cmH<sub>2</sub>O inflation pressure, and 2 cmH<sub>2</sub>O positive-end expiratory pressure (PEEP), consistent with the recommendations of Glaab et al. (11). PEEP is required to maintain functional residual capacity, as active inspiratory muscle tone is reduced in anesthetized mice (11). Animals were sequentially imaged at baseline and during two doses of continuous MCh infusion: 16  $\mu\text{g} \cdot \text{kg}^{-1} \cdot \text{min}^{-1}$  (MCh1) and subsequently, 48  $\mu\text{g} \cdot \text{kg}^{-1} \cdot \text{min}^{-1}$  (MCh2; Fig. 1). Each mouse was ventilated for at least 5 min before baseline measurements to allow it to stabilize after anesthetization and surgery. At least 5 min was allowed after instigation of the MCh1 and MCh2 infusions, before lung function and imaging, to allow the response to stabilize.

**Forced oscillation technique.** Lung mechanics were measured using a modification of the FOT, as described previously (12). Briefly, an oscillatory pressure signal containing nine frequencies, ranging from 4 to 38 Hz, was generated by a loudspeaker and delivered to the tracheal cannula by a wavetube of known impedance during 6-s pauses in ventilation. Lateral pressure transducers at the start of the wavetube and at the airway opening were used to calculate the respiratory system impedance spectrum (12). A four-parameter model with constant-phase tissue impedance was fitted to the respiratory system impedance spectrum to extract values for global airway resistance ( $R_{\text{aw}}$ ), tissue damping (G) and tissue elastance (H), and inductance (which is  $\sim 0$  after accounting for the tracheal cannula and not reported) (13).

**Imaging.** Imaging was conducted using a modification of the dynamic CT method, described in Dubsy et al. (7). Briefly, phase-contrast images were acquired at the SPring-8 synchrotron (Hyogo,

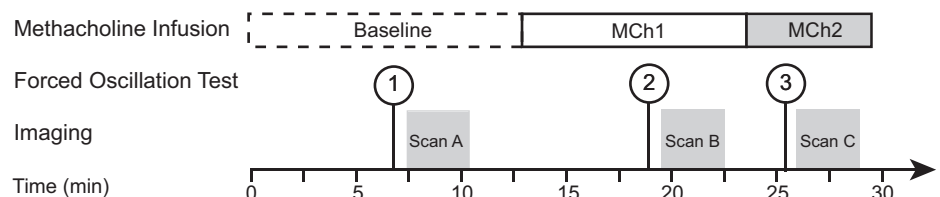
Japan) at the BL20B2 beamline. Images were acquired at 50 frames/s using a pco.edge sCMOS detector (PCO AG, Kelheim, Germany), optically coupled with a scintillator crystal. During imaging, the animal was placed upright in a custom-built holder, which was mounted on a five-axis motor controller to provide stable rotation during the 3-min scan. The ventilator provided stable, pressure-controlled ventilation and triggering to the imaging system for synchronization with the ventilation cycle. Single-image phase retrieval (21) and simultaneous algebraic reconstruction technique (2) were used for CT reconstruction. Imaging parameters resulted in high-resolution CT (HRCT) with an isotropic voxel size of 15  $\mu\text{m}$ . Airway size was measured at end-expiration at a ventilator pressure of 2 cmH<sub>2</sub>O.

**Airway size estimation and comparison.** Airway segmentation and size calculation were performed using a novel image-processing methodology, based on the vesselness filter described by Frangi et al. (9). This Hessian-based filter uses analysis of the eigenvalues of the image-intensity Hessian matrix at different spatial scales ( $\sigma$ ) to assign a probability value to each voxel. This value describes the probability of a cylinder (in our case, an airway) being present at each voxel. The spatial scale that yields the maximum vessel probability at any point may be used to estimate the vessel diameter (9, 24, 25). Values for  $\sigma$  corresponded to a diameter range of 85–950  $\mu\text{m}$ . The conversion from scale space (i.e.,  $\sigma$ ) to diameter was calibrated using synthetically generated images of cylinders of various lengths, as in Samarage et al. (25). These synthetically generated images were also used to estimate root mean square error in the diameter measurement in this range, which was shown to be 1.8 pixels. This is consistent with previous studies using scale-space diameter measurements, which achieved an accuracy of  $<5\%$  for diameters approximately  $>5$  pixels (8), as measured in the present study.

The four-dimensional CT images were processed using the vesselness filter to yield a vessel probability field. This was segmented using a floodfill, providing a binary image of the airway tree. Autoskeletonization (Aviso software; FEI, Hillsboro, OR) was then used to find the centerline of the airways. The scale of the vesselness filter that yielded the highest vessel probability at each centerline point of the airway tree was used as an estimate of the diameter of the airway at that point (Fig. 2). These estimates were averaged across each airway segment to yield the average diameter of each airway segment. This method provides robust, unsupervised diameter estimation across the entire airway tree, allowing for hundreds of airways down to a diameter of  $\sim 85$   $\mu\text{m}$  to be measured and compared for each animal (Fig. 3).

Airway segmentation methods are imperfect, leading to both missed and false airway segments (28). To compare automatically the diameters of airway segments between states, a simple multi-criteria airway matching was implemented. First, airway trees were coregistered to the baseline airway tree using a set of manually defined landmark points. Each point in the airway segment was then matched to the closest airway in the baseline tree. A segment match was accepted if two criteria were met:  $>60\%$  of points were consistently matched to an individual baseline airway, and its length was within 20% of that baseline airway. This prevented erroneous matching due to registration errors and/or missing airway segments.

Fig. 1. Study protocol. Mice were imaged at baseline and during 16  $\mu\text{g} \cdot \text{kg}^{-1} \cdot \text{min}^{-1}$  [methacholine (MCh1)] and 48  $\mu\text{g} \cdot \text{kg}^{-1} \cdot \text{min}^{-1}$  (MCh2) infusion. The forced oscillation technique was used to assess global lung mechanics immediately before each imaging scan.



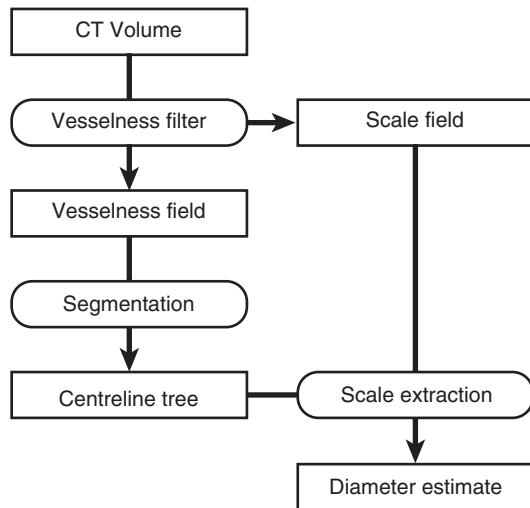


Fig. 2. Airway segmentation and centerline extraction process. The multiscale vesselness filter yields both the scale field and vesselness field. The airway tree was segmented from the vesselness field, and the centerline tree was extracted. The scale field was then interrogated at each point in the centerline tree to estimate the diameter of the airway at that point. This process results in a segmented airway tree with robust diameter estimation for all airways (as shown in Fig. 3).

## RESULTS

**Lung mechanics.** HDM-exposed mice exhibited a higher  $R_{aw}$  for all three conditions (baseline, MCh1, and MCh2:  $P = 0.048$ ; Fig. 4A) when compared with the CTL group. Both the HDM and CTL groups showed a paradoxical decrease in  $R_{aw}$  (representing the resistance of the conducting airways) for MCh1 challenge ( $P < 0.001$ ; Fig. 4A) and an increase in  $R_{aw}$  for the MCh2 challenge compared with baseline ( $P = 0.040$ ; Fig. 4A). No significant changes in  $G$  were observed between the HDM and CTL groups or for MCh1 ( $P = 0.43$  and  $P = 0.308$ , respectively; Fig. 4B). In contrast,  $G$  was significantly increased in response to MCh2 when compared with baseline and MCh1 ( $P = 0.029$  and  $P = 0.006$ , respectively; Fig. 4B).

There was no change in  $H$  in response to HDM compared with CTL mice ( $P = 0.43$ ) nor were there any changes in  $H$  in response to MCh1 or MCh2 challenges when compared with baseline ( $P = 0.499$ ; Fig. 4C).

**CT imaging.** Imaging provided CT reconstructions of sufficient quality and resolution to discern airways clearly from surrounding tissue (Fig. 5) of a size down to  $\sim 85 \mu\text{m}$ .

**Airway responses.** Scatter plots revealed the distribution of normalized airway response (airway diameter/baseline diameter) with respect to baseline diameter (Fig. 6, A–D). Friedman's super-smoother regression (10) was used to assess qualitatively the distribution of airway responses (Fig. 6, A–D). The lower limit on measurable size ( $85 \mu\text{m}$ ) resulted in apparent truncation of the data below a baseline diameter size of  $\sim 175 \mu\text{m}$ . This resulted in a bias in the regression toward a dilation response for baseline diameters below  $175 \mu\text{m}$ . For this reason, the fitting was extrapolated in this range, using a polynomial fit of order two, using data from a baseline diameter range of  $175\text{--}300 \mu\text{m}$ . All cases showed a large heterogeneity in response, with both dilating and constricting airways present. The distributions for CTL and HDM groups were similar (Fig. 6). All distributions showed an increased prevalence of para-

doxical dilation for larger airways, with increasing constriction for smaller airways. The mid-sized airways ( $\sim 300\text{--}500 \mu\text{m}$ ) showed the largest paradoxical dilation in response to MCh1.

In both HDM and CTL groups, for MCh1, the average diameter of airways, expressed as a percentage of baseline diameter, was  $>100\%$  (109% and 106%, respectively), indicating that on average, the measured airways dilated in response to MCh. For MCh2, the average response was  $<100\%$  from HDM and CTL groups (98% and 95%), indicating constriction. These results mirror the decreased  $R_{aw}$  for MCh1 and increased  $R_{aw}$  for MCh2.

The percentage of airways that dilated or constricted in specific size ranges allowed comparison of response distributions in response to MCh1 and MCh2 (Fig. 6, E and F). Generally, the number of dilating airways was highest in the range  $\sim 200\text{--}500 \mu\text{m}$  for MCh1 and generally increased with increasing baseline airway diameter for MCh2. The largest difference in dose response occurred in the mid-sized airways ( $\sim 200\text{--}500 \mu\text{m}$ ), which showed high percentages of dilating airways for MCh1 and only a moderate percentage of dilating airways for MCh2 in both HDM and CTL groups. The HDM group showed a greater prevalence of paradoxical dilation (42.1% and 68.2% for MCh1 and MCh2) than the CTL group (35.7% and 62.8%).

The response of individual airways under MCh1 and MCh2 challenges for both CTL and HDM groups showed moderate

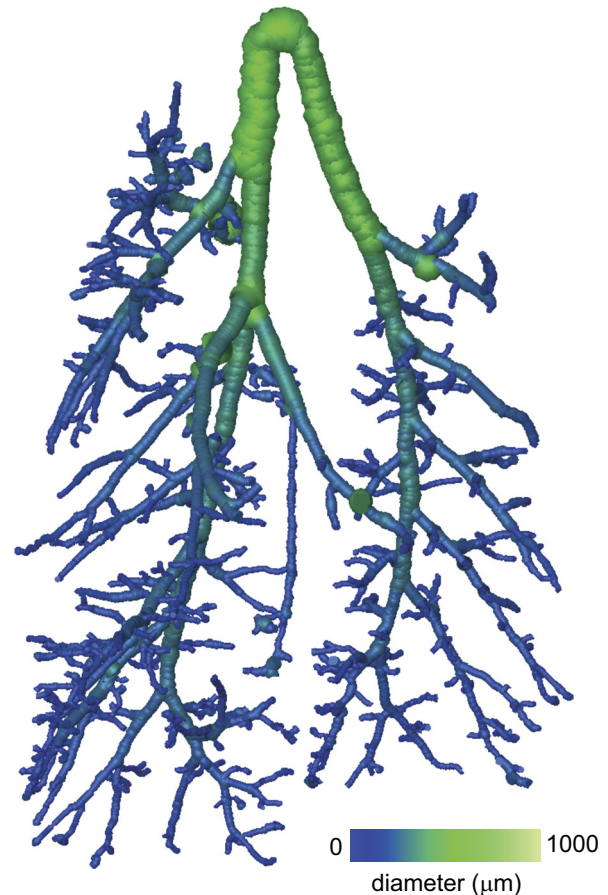


Fig. 3. Graphical representation of airway diameter measurement result. The airway tree is defined by a set of connected segments, each with a diameter and set of centerline points.

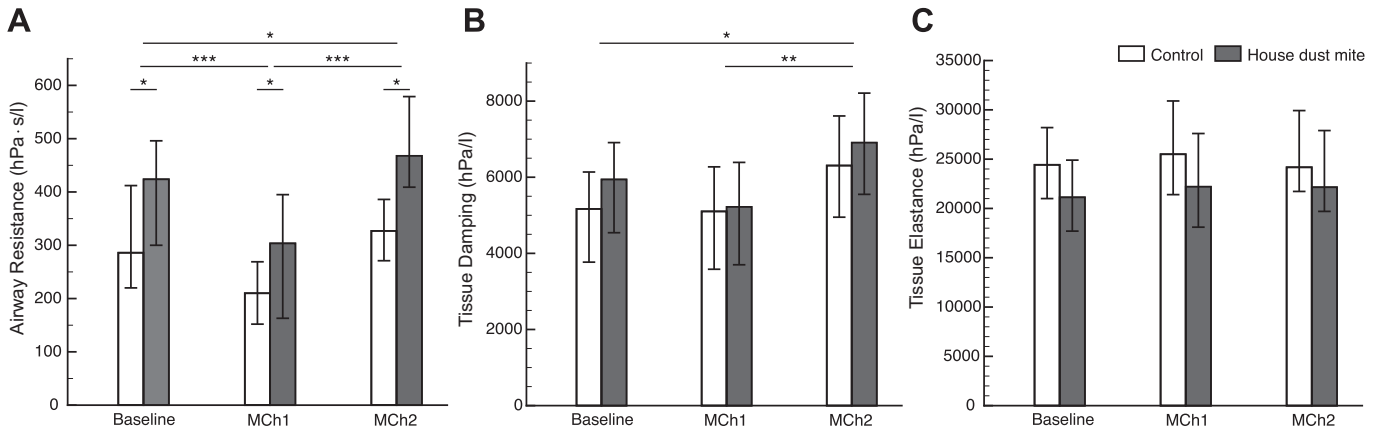


Fig. 4. Global lung mechanics measured using forced oscillation technique. Bars show average, and error bars indicate range. Results show paradoxical decrease in airway resistance for MCh1 ( $P < 0.001$ ) and increase for MCh2 ( $P = 0.04$ ). Resistance was higher at baseline in the HDM-exposed mice ( $P = 0.048$ ).  $*P < 0.05$ ,  $**P < 0.01$ ,  $***P < 0.001$ .

correlation (Pearson coefficient,  $R = 0.57$  and  $R = 0.56$ , respectively; Fig. 7), indicating a persistent pattern of response for MCh1 and MCh2 in both CTL and HDM groups.

## DISCUSSION

The results presented in this study demonstrate paradoxical dilation of airways in response to IV MCh in mice under positive pressure mechanical ventilation. Paradoxical dilation preferentially occurred in the larger airways, although it was present across all sizes of airways measured in this study (airway diameters  $>85 \mu\text{m}$ ). No significant difference in response distribution was seen between the HDM and CTL groups. However, the baseline resistance, measured by FOT, was significantly increased in the HDM group. Interestingly, a global paradoxical decrease in  $R_{\text{aw}}$  was also measured by the FOT during the MCh1 infusion in both HDM and CTL groups.

The presence of paradoxical dilation under bronchoconstriction has been identified previously in a number of studies. Brown et al. (4) used HRCT to measure airway response in canines exposed to inhaled histamine. A semi-automated pro-

cedure was used that enabled measurement of  $\sim 10$  airways in each subject. Results showed a marked heterogeneity in airway responses, including paradoxical dilation in one subject. Kotaru et al. (17) compared the response of airways in humans using HRCT under two different challenges: isocapnic hyperventilation of frigid air and inhaled MCh. Computer-assisted manual measurement of airway size was conducted from the trachea to the segmental bronchi (26 airways/subject). Imaging was conducted during a breath-hold at total lung capacity. All subjects showed a reduction in forced expiratory volume in 1 s after both challenges. The results demonstrated a large amount of heterogeneity, with both dilation and constriction present. In fact, only 47% of the airways measured constricted after MCh challenge. The frequency of dilation decreased with each generation, consistent with results from the present study. Bayat et al. (3) measured the response of airways in rabbits subjected to inhaled histamine challenge under two doses using synchrotron HRCT. The size of the main bronchi was measured in three axial planes between the apex and base of the lung, resulting in six measurements per subject. Results

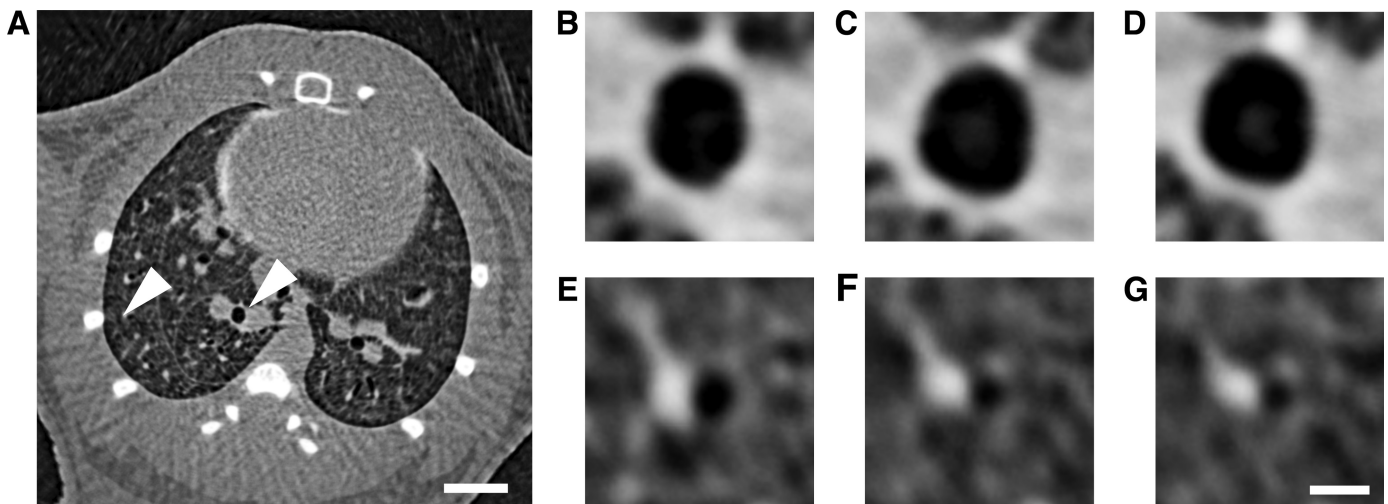


Fig. 5. Single CT slice (A) and zoomed images of individual airways at end-expiration for a large (B–D) and small (E–G) airway for baseline (B and E), methacholine (MCh)1 (C and F), and MCh2 (D and G). White arrowheads (A) indicate the 2 airways chosen for zoomed images (B–G). For the large airway, an increase in diameter is apparent for both the MCh1 and MCh2 challenge when compared with baseline, whereas the small airway shows progressive reduction in airway diameter under MCh challenge. Original scale bars, 2 mm (A) and  $250 \mu\text{m}$  (B–G; shown on G only).

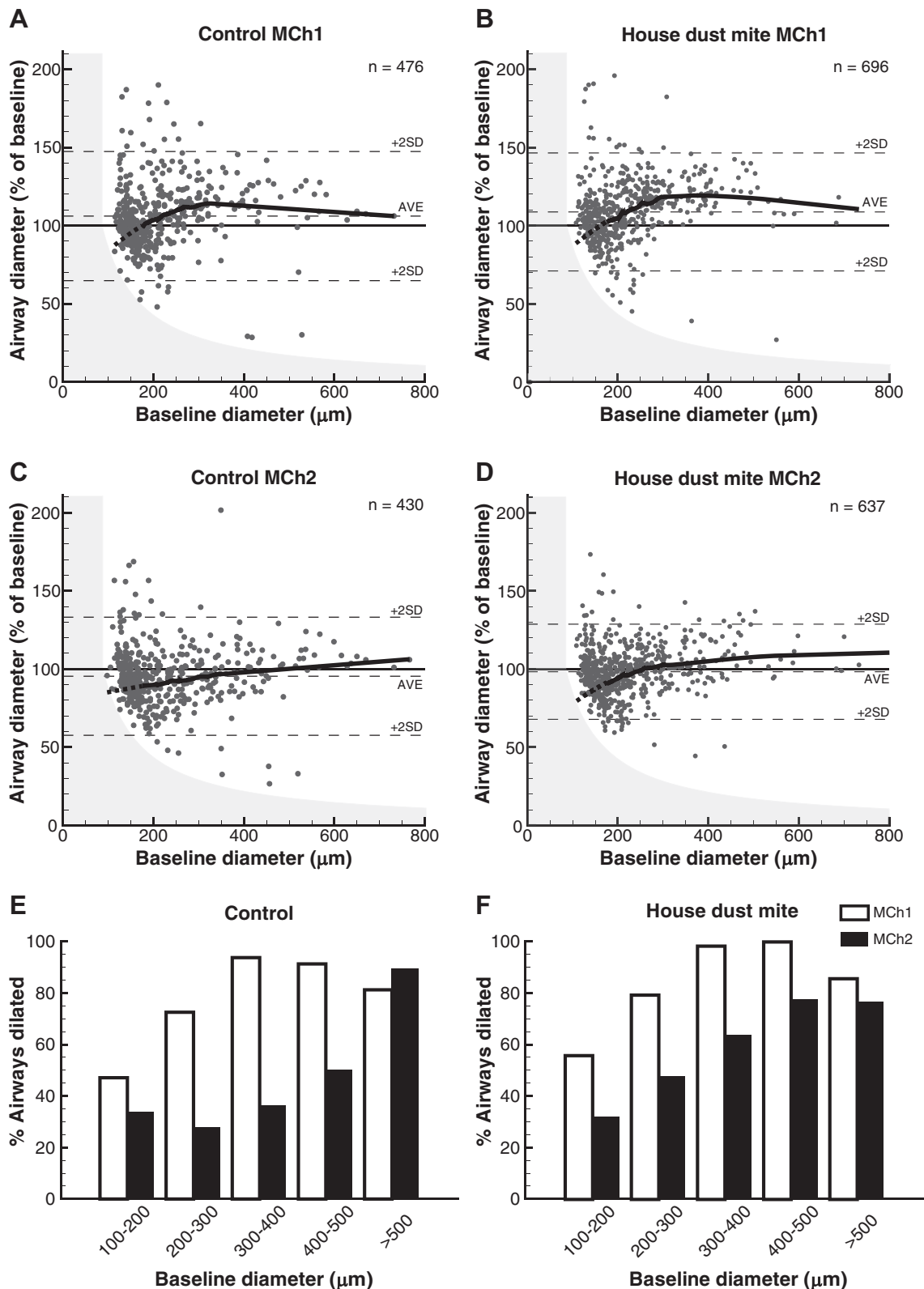


Fig. 6. Distribution of airway diameter in response to methacholine (MCh) challenge. Airway diameter distributions in response to MCh1 and MCh2 (A–D) and percentage of measured airways exhibiting dilation for specific size ranges (E and F). Friedman’s super-smoother regression is shown by the solid lines; dotted line shows extrapolation to account for truncation bias. The gray areas show regions in which airways are below measurable size. A clear proximal-to-distal distribution existed in all cases, with the larger airways showing paradoxical dilation in response to MCh challenge. Similar distributions were seen in both HDM-exposed and control mice.

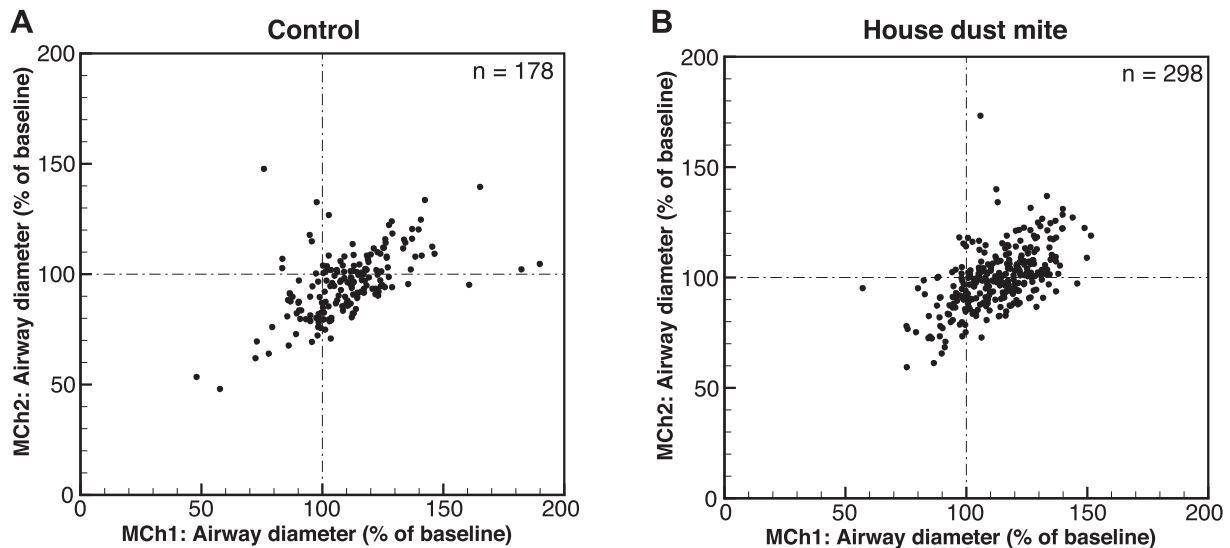


Fig. 7. Correlation of methacholine (MCh)1 and MCh2 airway response. Scatter plots of normalized airway diameter for individual airways under MCh1 vs. MCh2 challenge.

showed clear paradoxical airway dilation, with the extent of dilation generally increasing with the larger airways. No clear difference in response was apparent between the two doses used.

In our study, the FOT demonstrated significant changes in resistance but no change in H. Alterations in H result from either a change in tissue stiffness or may also be indicative of airway closure (15). This result indicates that all responses measured in this study were due to airway constriction and are unlikely to be a result of loss of lung units due to airway closure. It is possible that the upright position of the mice and the use of mechanical ventilation with PEEP of 2 cmH<sub>2</sub>O prevented airway closure during the experiments. In fact, the application of PEEP has been shown to reduce ventilation heterogeneity and improve alveolar ventilation during bronchoconstriction in both imaging (23) and modeling (29) studies, thus mitigating airway closure. The upright position will affect the longitudinal forces on the airways, which may alter airway-tissue interdependence when compared with the supine position. This may have an impact on regional constriction, possibly contributing to the unexpected decrease in  $R_{aw}$  apparent during MCh1. Position has been shown to have a significant effect on the regional response to MCh in humans (14).

The airway distributions measured in the present study are consistent with the findings of Kotaru et al. (17) and Bayat et al. (3), demonstrating that the likelihood of paradoxical dilation decreases from the larger airways to the smaller airways. This is in contrast to the findings of Brown et al. (4), who showed no clear relationship between airway size and measured response; however, the small number of airways measured in that study may have limited the ability to detect such a relationship given the large heterogeneities present.

We have identified dose dependence for paradoxical dilation, whereby the percentage of measured airways that dilate decreases with increasing MCh dose, in particular, in the mid-sized and larger airways. The contribution to total resistance decreases with each generation, as the number of airways, and hence, the total cross-sectional area increase rapidly with branching. Paradoxical dilation in the larger airways may

therefore reduce  $R_{aw}$ , even in the presence of constriction in smaller airways. This appears to be the case for MCh1, where this paradoxical dilation of the larger airways is most apparent. The results presented by Bayat et al. (3) do not show a clear difference between the responses to differing agonist dose. This may be due to the doses used or the limited number of airways measured (6 airway segments/subject). In any case, the correlation between responses from individual airways during the MCh1 and MCh2 challenges in our study indicates that a consistent factor drives individual airways to show a certain relative response. This is consistent with previous studies that have shown persistent locations for ventilation deficits in bronchoconstriction (5a). Modeling has suggested that the spatial persistence in response to bronchoconstriction may be due to airway tree asymmetry (19), which is particularly strong in the mouse lung.

The mechanisms that cause paradoxical dilation remain to be elucidated. The results in the literature, with regards to paradoxical dilation, are consistent across a number of animal species and challenges. The distribution of airway smooth muscle orientation within the airway tree is conserved across species, and the abundance of airway smooth muscle is increased in smaller distal airways (26). Therefore, airway smooth muscle distribution may be a possible contributing factor in the airway response distributions shown in our study. Most previous studies used an inhaled bronchoconstricting agent (3, 4, 17), which may lead to nonuniform delivery and may potentially contribute to the heterogeneous response. The present study used an IV delivery route, which is thought to deliver equal concentrations of MCh to the airway smooth muscle through the bronchial circulation (27). Route of delivery has been shown previously to affect the pattern of airway response to MCh in rabbits (27). However, the distributions measured in the present study are consistent with studies using inhaled delivery, demonstrating that the heterogeneities, due to uneven deposition of aerosols, are unlikely to be a strong contributing factor for the overall response distribution.

The distribution of response was consistently related to baseline airway size. This may imply a geometric factor that

contributes to paradoxical dilation. Interdependence effects have been shown to create paradoxical dilation in simplified computer models of airway constriction (29), and this may be a possible contributor to the paradoxical dilation shown in this study. The preferential dilation of larger airways would be consistent with a serial interdependence hypothesis. However, as the measurements in this study were acquired at end-expiration at a fixed expiratory pressure, dynamic internal pressure variations, due to serial interdependence, may not fully explain the results, and so some other factor, presumably physiological, may be present to cause persistent dilation of the airways. It is possible that a combination of airway geometry factors, such as serial interdependence combined with distribution of airway mechanical properties and airway structural components (e.g., airway smooth muscle, receptors, cartilage), causes paradoxical dilation to emerge during bronchoconstriction. Given the consistency in the observations between the HDM-exposed and CTL mice, it seems that prior inflammation has little impact on the heterogeneity of airway responses to bronchoconstricting agents. Further experiments to isolate the contribution of these factors to the distribution of airway constriction are warranted. It is hoped that the methods developed and response distributions measured in this study will contribute to these investigations.

#### ACKNOWLEDGMENTS

The authors gratefully acknowledge Jordan Thurgood and Richard Carnibella for assistance with the experiments.

#### GRANTS

Support for A. Fouras was provided by the National Health and Medical Research Council Career Development Fellowship (APP1022721). The project was supported by an American Asthma Foundation research grant, the Japan Synchrotron Radiation Research Institute (JASRI; 2012B1100), and the Multimodal Australian ScienceS Imaging and Visualisation Environment (MASSIVE; <https://www.massive.org.au/>), Australian Research Council (DP150102240).

#### DISCLOSURES

A. Fouras, S. Dubsky, C. R. Samarage, and Y. Henon hold beneficial interests in 4Dx Ltd., which commercializes respiratory diagnostics technology.

#### AUTHOR CONTRIBUTIONS

G.R.Z., K.P., S.B.H., and A.F. performed experiments; S.D., G.R.Z., C.R.S., and Y.H. analyzed data; S.D., G.R.Z., and A.F. interpreted results of experiments; S.D. prepared figures; S.D. drafted manuscript; S.D., G.R.Z., C.R.S., and S.B.H. edited and revised manuscript; S.D., G.R.Z., K.P., C.R.S., Y.H., S.B.H., and A.F. approved final version of manuscript.

#### REFERENCES

- Amin SD, Majumdar A, Frey U, Suki B. Modeling the dynamics of airway constriction: effects of agonist transport and binding. *J Appl Physiol* (1985) 109: 553–563, 2010. doi:10.1152/jappphysiol.01111.2009.
- Andersen AH, Kak AC. Simultaneous algebraic reconstruction technique (SART): a superior implementation of the art algorithm. *Ultrason Imaging* 6: 81–94, 1984. doi:10.1177/016173468400600107.
- Bayat S, Porra L, Suhonen H, Suortti P, Sovijärvi ARA. Paradoxical conducting airway responses and heterogeneous regional ventilation after histamine inhalation in rabbit studied by synchrotron radiation CT. *J Appl Physiol* (1985) 106: 1949–1958, 2009. doi:10.1152/jappphysiol.90550.2008.
- Brown RH, Herold CJ, Hirshman CA, Zerhouni EA, Mitzner W. In vivo measurements of airway reactivity using high-resolution computed tomography. *Am Rev Respir Dis* 144: 208–212, 1991. doi:10.1164/ajrcm/144.1.208.
- Chew AD, Hirota JA, Ellis R, Wattie J, Inman MD, Janssen LJ. Effects of allergen on airway narrowing dynamics as assessed by lung-slice technique. *Eur Respir J* 31: 532–538, 2008. doi:10.1183/09031936.00079307.
- de Lange EE, Altes TA, Patrie JT, Parmar J, Brookeman JR, Mugler JP III, Platts-Mills TAE. The variability of regional airflow obstruction within the lungs of patients with asthma: assessment with hyperpolarized helium-3 magnetic resonance imaging. *J Allergy Clin Immunol* 119: 1072–1078, 2007. doi:10.1016/j.jaci.2006.12.659.
- Donovan C, Royce SG, Esposito J, Tran J, Ibrahim ZA, Tang MLK, Bailey S, Bourke JE. Differential effects of allergen challenge on large and small airway reactivity in mice. *PLoS One* 8: e74101, 2013. doi:10.1371/journal.pone.0074101.
- Dubsky S, Hooper SB, Siu KKW, Fouras A. Synchrotron-based dynamic computed tomography of tissue motion for regional lung function measurement. *J R Soc Interface* 9: 2213–2224, 2012. doi:10.1098/rsif.2012.0116.
- Estépar RS, Ross JC, Russian K, Schultz T, Washko GR, Kindlmann GL. Computational vascular morphometry for the assessment of pulmonary vascular disease based on scale-space particles. *Proc IEEE Int Symp Biomed Imaging* 1479–1482, 2012.
- Frangi AF, Niessen WJ, Vincken KL, Viergever MA. Multiscale vessel enhancement filtering. In: *International Conference on Medical Image Computing and Computer-Assisted Intervention*. Berlin Heidelberg: Springer, 2016, p. 130–137.
- Friedman JH. *A Variable Span Smoother. Technical Report No. 5*. Stanford, CA: Dept. of Statistics, Stanford University, 1984.
- Glaab T, Taube C, Braun A, Mitzner W. Invasive and noninvasive methods for studying pulmonary function in mice. *Respir Res* 8: 63, 2007. doi:10.1186/1465-9921-8-63.
- Hantos Z, Collins RA, Turner DJ, Jánosi TZ, Sly PD. Tracking of airway and tissue mechanics during TLC maneuvers in mice. *J Appl Physiol* (1985) 95: 1695–1705, 2003. doi:10.1152/jappphysiol.00104.2003.
- Hantos Z, Daróczy B, Suki B, Nagy S, Fredberg JJ. Input impedance and peripheral inhomogeneity of dog lungs. *J Appl Physiol* (1985) 72: 168–178, 1992.
- Harris RS, Winkler T, Musch G, Vidal Melo MF, Schroeder T, Tgavalekos N, Venegas JG. The prone position results in smaller ventilation defects during bronchoconstriction in asthma. *J Appl Physiol* (1985) 107: 266–274, 2009. doi:10.1152/jappphysiol.91386.2008.
- Irvin CG, Bates JH. Measuring the lung function in the mouse: the challenge of size. *Respir Res* 4: 4, 2003. doi:10.1186/rr199.
- Kitchen MJ, Habib A, Fouras A, Dubsky S, Lewis RA, Wallace MJ, Hooper SB. A new design for high stability pressure-controlled ventilation for small animal lung imaging. *J Instrum* 5: T02002, 2010. doi:10.1088/1748-0221/5/02/T02002.
- Kotaru C, Coreno A, Skowronski M, Muswick G, Gilkeson RC, McFadden ER Jr. Morphometric changes after thermal and methacholine bronchoprovocations. *J Appl Physiol* (1985) 98: 1028–1036, 2005. doi:10.1152/jappphysiol.01186.2003.
- Leary D, Winkler T, Braune A, Maksym GN. Effects of airway tree asymmetry on the emergence and spatial persistence of ventilation defects. *J Appl Physiol* (1985) 117: 353–362, 2014. doi:10.1152/jappphysiol.00881.2013.
- Noble PB, McFawn PK, Mitchell HW. Responsiveness of the isolated airway during simulated deep inspirations: effect of airway smooth muscle stiffness and strain. *J Appl Physiol* (1985) 103: 787–795, 2007. doi:10.1152/jappphysiol.00314.2007.
- Paganin D, Mayo SC, Gureyev TE, Miller PR, Wilkins SW. Simultaneous phase and amplitude extraction from a single defocused image of a homogeneous object. *J Microsc* 206: 33–40, 2002. doi:10.1046/j.1365-2818.2002.01010.x.
- Politi AZ, Donovan GM, Tawhai MH, Sanderson MJ, Lauzon A-M, Bates JHT, Sneyd J. A multiscale, spatially distributed model of asthmatic airway hyper-responsiveness. *J Theor Biol* 266: 614–624, 2010. doi:10.1016/j.jtbi.2010.07.032.
- Porra L, Suhonen H, Suortti P, Sovijärvi ARA, Bayat S. Effect of positive end-expiratory pressure on regional ventilation distribution during bronchoconstriction in rabbit studied by synchrotron radiation imaging. *Crit Care Med* 39: 1731–1738, 2011. doi:10.1097/CCM.0b013e318218a375.
- Rudyanto RD, Ortiz de Solórzano C, Muñoz-Barrutia A. Quantification of pulmonary vessel diameter in low-dose CT images. *Proc SPIE, Medical Imaging 2015: Computer-Aided Diagnosis* 9414: 94142U, 2015.
- Samarage CR, Carnibella R, Preissner M, Jones HD, Pearson JT, Fouras A, Dubsky S. Technical note: Contrast free angiography of the

- pulmonary vasculature in live mice using a laboratory x-ray source. *Med Phys* 43: 6017–6023, 2016. doi:[10.1118/1.4964794](https://doi.org/10.1118/1.4964794).
26. **Smiley-Jewell SM, Tran MU, Weir AJ, Johnson ZA, Van Winkle LS, Plopper CG.** Three-dimensional mapping of smooth muscle in the distal conducting airways of mouse, rabbit, and monkey. *J Appl Physiol (1985)* 93: 1506–1514, 2002. doi:[10.1152/jappphysiol.01109.2001](https://doi.org/10.1152/jappphysiol.01109.2001).
27. **Strengell S, Porra L, Sovijärvi A, Suhonen H, Suortti P, Bayat S.** Differences in the pattern of bronchoconstriction induced by intravenous and inhaled methacholine in rabbit. *Respir Physiol Neurobiol* 189: 465–472, 2013. doi:[10.1016/j.resp.2013.08.024](https://doi.org/10.1016/j.resp.2013.08.024).
28. **Tschirren J, McLennan G, Palágyi K, Hoffman EA, Sonka M.** Matching and anatomical labeling of human airway tree. *IEEE Trans Med Imaging* 24: 1540–1547, 2005. doi:[10.1109/TMI.2005.857653](https://doi.org/10.1109/TMI.2005.857653).
29. **Winkler T, Venegas JG.** Complex airway behavior and paradoxical responses to bronchoprovocation. *J Appl Physiol (1985)* 103: 655–663, 2007. doi:[10.1152/jappphysiol.00041.2007](https://doi.org/10.1152/jappphysiol.00041.2007).

